Support motion of a finite bar with a viscously damped boundary

Jeng-Tzong Chen [1,2,3,4,5,*], Hao-Chen Kao[1], Jia-Wei Lee [6] and Ying-Te Lee[1]

[1]Department of Harbor and River Engineering, National Taiwan Ocean University, Keelung, Taiwan
[2]Department of Mechanical and Mechatronic Engineering, National Taiwan Ocean University, Keelung, Taiwan
[3]Department of Civil Engineering, National Taiwan University, Taipei, Taiwan
[4]Department of Civil Engineering, National Cheng Kung University, Tainan, Taiwan
[5]Center of Excellence for Ocean Engineering, National Taiwan Ocean University, Keelung, Taiwan
[6]Department of Civil Engineering, Tamkang University, New Taipei City, Taiwan

*Corresponding author: jtchen@mail.ntou.edu.tw

ABSTRACT

In this paper, we extended the previous experience to solve the vibration problem of a finite bar with a viscously damped boundary and the support motion on the other side. Two analytical methods, the mode superposition method in conjunction with the quasi-static decomposition method and the method of diamond rule based on the method of characteristics, were employed to derive two analytical solutions. One is a series solution by using the mode superposition method. The other is an exact solution by using the method of diamond rule. The non-conservative system with an external damper is solved straightforward by using the method of diamond rule to avoid the complex-valued eigen system. Agreement is made well. Both advantages and disadvantages of two methods were discussed.

KEYWORDS: support motion, viscous damper, mode superposition method, quasi-static decomposition, diamond rule

1. INTRODUCTION

Simulation of support motion is very important in physics and engineering, because there are various engineering problems for buildings, cars and equipment which can be modeled by using this model. Many researchers have solved this problem by using various methods, e.g. the mode superposition technique [1], the method of separation variables [2–4], the method of quasi-static decomposition [3, 5, 6], the method of the diamond rule [3, 7] or the so-called method of characteristics, the image method [6], the finite element method (FEM) [8], the boundary element method (BEM) [9], the meshless method [10], etc.

The Rayleigh-damped Bernoulli-Euler beam and the string subjected to multi-support excitation have been studied by using many methods including Stokes transformation and Cesaro sum [3, 5, 6]. For the Euler beam, Su and Cho [11] studied the free vibration of a single-walled carbon nanotube based on the nonlocal Timoshenko beam mode. Besides, nonlinear effect is an interesting and practical issue. Lin *et al.* [12] studied the nonlinear free vibration of size-dependent microbeams with nonlinear elasticity under various boundary conditions. Hull [2] and Jovanovic [13] solved the rod and beam problems with a viscous boundary, respectively. They faced the non-self-adjoint operator and orthogonality condition of complex modes needs special care. Jovanovic also extended to the torsion damper [14]. Two ends of dampers were also investigated and the stability was also discussed by Udawadia [15] and Jovanovic [16]. A beam including the internal damping in span and a boundary damper was studied by Gurgoze and Erol [17].

Since a viscous damper is very popular to reduce the earthquake response, support motion is also the main concern of this paper. Exact solutions for a system with an external damper are sparse. Results of continuous and discrete systems were compared with by Singh *et al.* [3]. Besides, a case of the limiting damping was also discussed. Although Hull [2] claimed that he derived a closed-form solution and compared with FEM well, the solution was a series solution instead of an exact solution. In addition, he showed only a frequency domain example of a concentrated dynamic loading.

The D'Alembert's solution can provide an exact solution for an infinite string. Method of characteristics (Diamond rule) can be found in the textbook of Farlow [18]. It is widely employed to solve various kinds of problems, e.g. water hammer [19]. The diamond rule on the D'Alembert's solution was proposed by John [20] in 1975 and was popularly used to solve the wave problem. The diamond rule has been employed to solve the one-dimensional vibration problem of an infinite or a semi-infinite string attached by a mass, a spring, or a damper [7], a finite string [3] and a finite bar with an external spring subjected to a support motion [5]. Besides, the animation was also given in [7]. Although the mode superposition method in conjunction with the quasi-static decomposition is a general approach for solving the support-motion problem, it becomes tedious when the vibration system contains a damper. Three reasons can be explained. One is that the quasi-static solution is not easily obtained straightforward for the support motion. Another
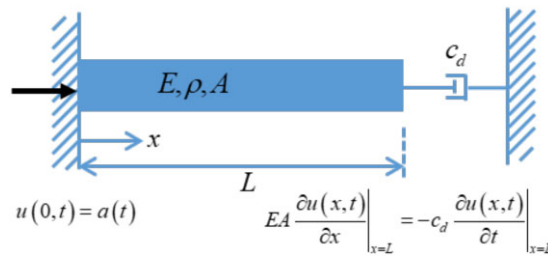
Figure 1 Sketch of a finite bar with a viscously damped boundary subjected to a support motion.

is that the orthogonal relation of complex modes is not obviously found. The other is that a complex eigen system is required. The present solution free of mode superposition is possible since we can employ the method of characteristics in conjunction with the diamond rule for the real response in the time domain. To yield an exact solution in the time domain is the main focus of this paper. Mode superposition of series solution using complex eigenmodes can be employed to check our solution.

In this paper, we extend the vibration problem of a finite bar with an external spring [4] to a finite bar with an external viscous damper. For the non-conservative system with an external viscous damper, two analytical solutions are obtained.

2. PROBLEM STATEMENTS AND METHODS OF SOLUTION

Here, we consider a finite bar with a viscously damped boundary as shown in Fig. 1. The governing equation for the vibration problem of a finite bar is as follows:

$$c^2 \frac{\partial^2 u(x, t)}{\partial x^2} = \frac{\partial^2 u(x, t)}{\partial t^2}, \, 0 < x < L, t > 0, \tag{1}$$

where $c = \sqrt{EA/\rho}$ and $u(x, t)$ denote the wave speed and displacement in the x direction, respectively. The symbols E, A, ρ and L denote Young's modulus, the area of cross section, the mass per unit length and the length of bar, respectively. The initial displacement and velocity conditions are as follows:

$$u(x, t)\big|_{t=0} = \phi(x) = 0, \tag{2}$$

$$\frac{\partial u(x, t)}{\partial t}\bigg|_{t=0} = \varphi(x) = 0, \tag{3}$$

where $\phi(x)$ and $\varphi(x)$ are initial displacement and velocity functions, respectively.

The boundary condition at the left-hand side ($x = 0$) can be expressed by the specified support motion as follows:

$$u(0, t) = a(t). \tag{4}$$

The boundary condition at the right-hand side is given by the viscous damper in Fig. 1 as follows:

$$EA \frac{\partial u(x, t)}{\partial x}\bigg|_{x=L} = -c_d \frac{\partial u(x, t)}{\partial t}\bigg|_{x=L}, \tag{5}$$

where c_d denotes the damping coefficient.

2.1 Method 1: Mode superposition approach in conjunction with the quasi-static decomposition method

The solution can be decomposed into two parts:

$$u(x, t) = U(x, t) + \sum_{n=-\infty}^{\infty} q_n(t) u_n(x), \tag{6}$$

where $U(x, t)$ denotes the quasi-static solution, $u_n(x)$ is the natural mode and $q_n(t)$ is the generalized coordinates of dynamic contribution due to the inertia effect. The quasi-static part $U(x, t)$ satisfies the governing equation,

$$EA \frac{\partial^2 U(x, t)}{\partial x^2} = 0, \, 0 < x < L, \tag{7}$$

and is subject to time-dependent boundary conditions at the two sides:

$$U(0, t) = a(t), \tag{8}$$

$$EA \left. \frac{\partial U\left(x,t\right)}{\partial x}\right|_{x=L} = -c_d \left. \frac{\partial U\left(x,t\right)}{\partial t}\right|_{x=L}. \tag{9}$$

By solving Eq. (7) to satisfy the boundary conditions, we have the quasi-static solution,

$$U\left(x,t\right) = \alpha\left(t\right)x + \beta\left(t\right), \tag{10}$$

where

$$\alpha\left(t\right) = e^{-\frac{AE}{c_d L}t}\left[\int_0^t -e^{\frac{AE}{c_d L}\tau}\frac{\dot{a}\left(\tau\right)}{L}d\tau + C\right], \tag{11}$$

$$\beta\left(t\right) = a\left(t\right), \tag{12}$$

after using the integration factor, where the undetermined constant, C, can be determined by

$$\alpha\left(0\right) = a\left(0\right). \tag{13}$$

The nth complex-valued function, $u_n(x)$, with the corresponding complex-valued eigenvalue λ_n is

$$u_n\left(x\right) = e^{\lambda_n x} - e^{-\lambda_n x}, n = 0, \pm 1, \pm 2, \cdots, \tag{14}$$

The corresponding complex-valued eigenvalues are given as follows:

$$\lambda_n = -\frac{1}{2L}\ln\left(\frac{c_d c + EA}{c_d c - EA}\right) - \frac{n\pi}{L}i, n = 0, \pm 1, \pm 2, \cdots, \tag{15}$$

and the corresponding complex-valued angular frequencies are as follows:

$$\omega_n = c\lambda_n, n = 0, \pm 1, \pm 2\cdots. \tag{16}$$

The detail derivation of Eq. (15) is presented in the Appendix.

To derive the governing equations of generalized coordinates $q_n(t)$, we follow the Hull's work [2]. The main difference is that we consider the support motion instead of body source excitation in [2]. To differentiate Eq. (6) with respect to t, we have

$$\frac{\partial u\left(x,t\right)}{\partial t} = \dot{U}\left(x,t\right) + \sum_{n=-\infty}^{\infty} \dot{q}_n\left(t\right)u_n\left(x\right). \tag{17}$$

By using Eqs. (A8) and (A4) (in the Appendix), Eq. (17) can be written as

$$\frac{\partial u\left(x,t\right)}{\partial t} = \dot{U}\left(x,t\right) + \sum_{n=-\infty}^{\infty} \omega_n q_n\left(t\right)u_n\left(x\right). \tag{18}$$

By subtracting Eq. (18) from Eq. (17), we have

$$\sum_{n=-\infty}^{\infty} \left[\dot{q}_n\left(t\right) - \omega_n q_n\left(t\right)\right]\left(e^{\lambda_n x} - e^{-\lambda_n x}\right) = 0. \tag{19}$$

By differentiating Eq. (19) with respect to x and multiplying by the wave speed c, we obtain

$$\sum_{n=-\infty}^{\infty} \left[\dot{q}_n\left(t\right) - \omega_n q_n\left(t\right)\right]\omega_n\left(e^{\lambda_n x} + e^{-\lambda_n x}\right) = 0. \tag{20}$$

Similarly, substituting Eq. (6) into Eq. (1) and using Eqs. (A8) and (A4), we have

$$\sum_{n=-\infty}^{\infty} \left[\dot{q}_n\left(t\right) - \omega_n q_n\left(t\right)\right]\omega_n\left(e^{\lambda_n x} - e^{-\lambda_n x}\right) = -\ddot{U}\left(x,t\right). \tag{21}$$

In this way, the governing equations of generalized coordinates $q_n(t)$ can be decoupled by using Eq. (20) and Eq. (21). By adding Eq. (20) to Eq. (21) together and subtracting Eq. (20) from Eq. (21), we obtain

$$\sum_{n=-\infty}^{\infty} \left[\dot{q}_n\left(t\right) - \omega_n q_n\left(t\right)\right]2\omega_n e^{\lambda_n x} = -\ddot{U}\left(x,t\right), x \in [0,L] \tag{22}$$

and

$$\sum_{n=-\infty}^{\infty} [\dot{q}_n(t) - \omega_n q_n(t)] 2\omega_n e^{-\lambda_n x} = \ddot{U}(x, t), \, x \in [0, L],$$ (23)

respectively. In Eq. (23), x is replaced by $-x$ and the interval is changed from $[0, L]$ to $[-L, 0]$, we have

$$\sum_{n=-\infty}^{\infty} [\dot{q}_n(t) - \omega_n q_n(t)] 2\omega_n e^{\lambda_n x} = \ddot{U}(-x, t), \, x \in [-L, 0].$$ (24)

Substituting the complex-valued eigenvalue into Eqs. (22) and (24) and rearranging them into a single equation, we have

$$\sum_{n=-\infty}^{\infty} [\dot{q}_n(t) - \omega_n q_n(t)] 2\omega_n e^{\frac{-n\pi}{L}ix} = \begin{cases} -e^{\frac{1}{2L}\ln\left(\frac{c_d c + EA}{c_d c - EA}\right)x}\ddot{U}(x, t), \, x \in [0, L] \\ e^{\frac{1}{2L}\ln\left(\frac{c_d c + EA}{c_d c - EA}\right)x}\ddot{U}(-x, t), \, x \in [-L, 0] \end{cases}.$$ (25)

Eq. (27) gives us a Fourier series expansion for orthogonal bases of $e^{-n\pi ix/L}$ with respect to the interval of $[-L, L]$.
Multiplying the exponential term $e^{m\pi ix/L}$ (where m is an integer) on both sides of Eq. (25) and integrating from $-L$ to L, the left side of Eq. (25) can be expressed as follows:

$$\int_{-L}^{L} [\dot{q}_n(t) - \omega_n q_n(t)] 2\omega_n e^{\frac{-n\pi}{L}ix} e^{\frac{m\pi}{L}ix} dx = \begin{cases} 4[\dot{q}_n(t) - \omega_n q(t)] \omega_n L, \, m = n \\ 0, \, m \neq n \end{cases}$$ (26)

For the right side of Eq. (25), it can be combined by using the reflection property of integrals as given below:

$$\int_0^L -e^{-\lambda_n x}\ddot{U}(x, t)\,dx + \int_{-L}^0 e^{-\lambda_n x}\ddot{U}(-x, t)\,dx = \int_0^L u_n(x)\ddot{U}(x, t)\,dx.$$ (27)

Combining Eqs. (26) and (27), the first-order ordinary differential equation for the generalized coordinates $q_n(t)$ can be obtained as

$$\dot{q}_n(t) - \omega_n q_n(t) = \frac{1}{4\omega_n L} \int_0^L u_n(x)\ddot{U}(x, t)\,dx.$$ (28)

The initial condition of generalized coordinates can be determined from the initial conditions of the total solution. Using Eq. (6) to satisfy the initial displacement condition in Eq. (2) and differentiating it with respect to x, we have

$$\left.\frac{\partial u(x, t)}{\partial x}\right|_{t=0} = \frac{\partial \phi(x)}{\partial x} = 0 = U'(x, 0) + \sum_{n=-\infty}^{\infty} q_n(0) \lambda_n \left(e^{\lambda_n x} + e^{-\lambda_n x}\right).$$ (29)

Multiplying Eq. (29) by the wave speed c, we have

$$\sum_{n=-\infty}^{\infty} \omega_n q_n(0) \left(e^{\lambda_n x} + e^{-\lambda_n x}\right) = -cU'(x, 0).$$ (30)

Similarly, using Eq. (6) to satisfy the initial velocity condition in Eq. (3), we have

$$\left.\frac{\partial u(x, t)}{\partial t}\right|_{t=0} = \varphi(x) = 0 = \dot{U}(x, 0) + \sum_{n=-\infty}^{\infty} \omega_n q_n(0) \left(e^{\lambda_n x} - e^{-\lambda_n x}\right).$$ (31)

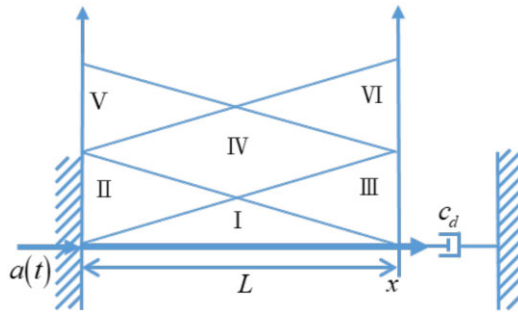By adding Eq. (31) to Eq. (30) together and subtracting Eq. (31) from Eq. (30), we obtain

$$\sum_{n=-\infty}^{\infty} \omega_n q_n(0) 2e^{\lambda_n x} = -cU'(x, 0) - \dot{U}(x, 0), \, x \in [0, L]$$ (32)

and

$$\sum_{n=-\infty}^{\infty} \omega_n q_n(0) 2e^{-\lambda_n x} = -cU'(x, 0) + \dot{U}(x, 0), \, x \in [0, L],$$ (33)

respectively. In Eq. (33), x is replaced by $-x$ and the interval is changed from $[0, L]$ to $[-L, 0]$, we have

$$\sum_{n=-\infty}^{\infty} \omega_n q_n(0) 2e^{\lambda_n x} = -cU'(-x, 0) + \dot{U}(-x, 0), \, x \in [-L, 0].$$ (34)

Figure 2 Space-time regions separated by using the characteristic line.

Similarly, combining Eqs. (32) and (34) into a single equation and rearranging it, we have

$$\sum_{n=-\infty}^{\infty} 2\omega_n q_n (0) e^{\frac{-n\pi}{L} ix} = \begin{cases} e^{\frac{1}{2L} \ln\left(\frac{c_d c + EA}{c_d c - EA}\right) x} \left[-c\, U'(x, 0) - \dot{U}(x, 0)\right], x \in [0, L] \\ e^{\frac{1}{2L} \ln\left(\frac{c_d c + EA}{c_d c - EA}\right) x} \left[-c\, U'(-x, 0) + \dot{U}(-x, 0)\right], x \in [-L, 0] \end{cases}. \tag{35}$$

Multiplying the exponential term $e^{m\pi ix/L}$ (where m is an integer) on both sides of Eq. (35) and integrating from $-L$ to L, the left side of Eq. (35) can be expressed as

$$\int_{-L}^{L} \omega_n q_n (0) 2 e^{\frac{-n\pi}{L} ix} e^{\frac{m\pi}{L} ix} dx = \begin{cases} 4 q_n (0) \omega_n L, & m = n \\ 0, & m \neq n \end{cases}. \tag{36}$$

Using of the reflection property of integrals in the right side of Eq. (35), we have

$$\int_0^L e^{-\lambda_n x} \left[-c\, U'(x, 0) - \dot{U}(x, 0)\right] dx + \int_{-L}^0 e^{-\lambda_n x} \left[-c\, U'(-x, 0) + \dot{U}(-x, 0)\right] dx$$

$$= -\int_0^L c\, U'(x, 0) \left(e^{\lambda_n x} + e^{-\lambda_n x}\right) dx + \int_0^L \dot{U}(x, 0) u_n(x) dx. \tag{37}$$

Combining Eqs. (36) and (37), the initial condition of generalized coordinates, $q_n(0)$, can be obtained as

$$q_n (0) = \frac{-1}{4\lambda_n L} \int_0^L U'(x, 0) \left(e^{\lambda_n x} + e^{-\lambda_n x}\right) dx + \frac{1}{4\omega_n L} \int_0^L \dot{U}(x, 0) u_n(x) dx. \tag{38}$$

Therefore, we can solve $q_n(t)$ by considering Eqs. (28) and (38) and have

$$q_n (t) = \frac{e^{ct\lambda_n}}{2cL\lambda_n^3} \left[\int_0^t e^{-c\lambda_n \tau} \left(\lambda_n \left(-1 + \cosh(\lambda_n L) a''(\tau)\right) + \left(\lambda_n L \cosh(\lambda_n L) - \sinh(\lambda_n L)\right) \alpha''(\tau)\right) d\tau \right.$$

$$\left. -\lambda_n a'(0) + \sinh(\lambda_n L) \left(c\lambda_n \alpha(0) - \alpha'(0)\right) + \lambda_n \cosh(\lambda_n L) \left(a'(0) + L\alpha'(0)\right) \right] \tag{39}$$

Finally, the series solution for the displacement, $u(x, t)$, is as follows:

$$u(x, t) = U(x, t) + \sum_{n=-\infty}^{\infty} q_n(t) \left(e^{\lambda_n x} - e^{-\lambda_n x}\right). \tag{40}$$

2.2 Method 2: Method of characteristics in conjunction with the diamond rule

The general solution of 1D wave equation can be obtained by using the method of characteristic line and we have

$$u(x, t) = P(x + ct) + Q(x - ct), \tag{41}$$

where $P(x + ct)$ and $Q(x - ct)$ stand for a left-going-traveling wave and a right-going-traveling wave, respectively. By using two characteristic lines, $x + ct = 0$ and $x - ct = 0$, the space-time region can be decomposed into several division as shown in Fig. 2. Each region in Fig. 2 is a parallelogram or an isosceles triangle. After using Eq. (41) to satisfy the initial conditions in Eqs. (2) and (3), we have the D'Alembert's solution for the region I

$$u(x, t) = \frac{1}{2} \left[\phi(x + ct) + \phi(x - ct)\right] + \frac{1}{2c} \int_{x-ct}^{x+ct} \varphi(\tau) d\tau, \tag{42}$$
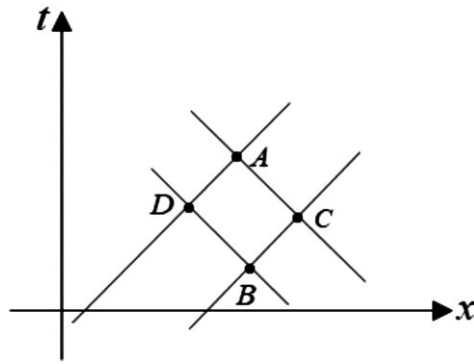
Figure 3 The diamond rule of $u_A + u_B = u_C + u_D$.
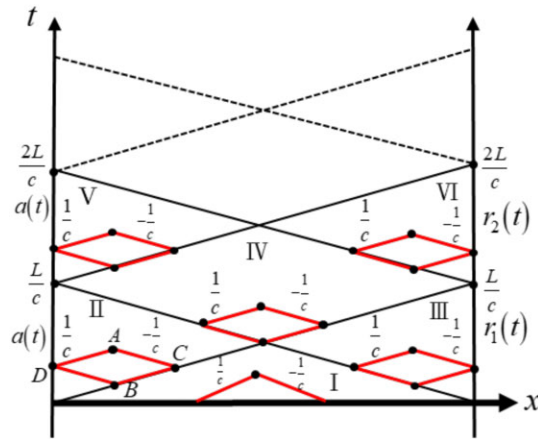

Figure 4 Space-time regions, I, II, III, IV, V and VI and the diamond rule.

where $\phi(\cdot)$ and $\varphi(\cdot)$ are initial displacement and velocity functions, respectively. According to the property of the D'Alembert's solution, we have the relationship between the displacements at the four vertices of a diamond as follows:

$$u_A + u_B = u_C + u_D, \tag{43}$$

where u_A, u_B, u_C and u_D denote the displacement at the four points A, B, C and D, respectively as shown in Fig. 3. It is noted that any side of a diamond is parallel to a certain characteristic line. Eq. (43) is the so-called diamond rule [4, 7]. We can employ the space-time marching scheme in Eq. (45) to calculate the displacement response for any time and space. By using the diamond rule for the former six regions as shown in Fig. 4, the displacements can be expressed as

$$u_{\mathrm{I}}(x, t) = 0, \ (x, t) \in \mathrm{I}, \tag{44}$$

$$u_{\mathrm{II}}(x, t) = a\left(\frac{ct - x}{c}\right), \ (x, t) \in \mathrm{II}, \tag{45}$$

$$u_{\mathrm{III}}(x, t) = r_1\left(\frac{x + ct - L}{c}\right), \ (x, t) \in \mathrm{III}, \tag{46}$$

$$u_{\mathrm{IV}}(x, t) = r_1\left(\frac{x + ct - L}{c}\right) + a\left(\frac{ct - x}{c}\right), \ (x, t) \in \mathrm{IV}, \tag{47}$$

$$u_{\mathrm{V}}(x, t) = r_1\left(\frac{x + ct - L}{c}\right) + a\left(\frac{ct - x}{c}\right) - r_1\left(\frac{ct - x - L}{c}\right), \ (x, t) \in \mathrm{V}, \tag{48}$$

$$u_{VI}(x, t) = a\left(\frac{ct - x}{c}\right) - a\left(\frac{x + ct - 2L}{c}\right) + r_2\left(\frac{x + ct - L}{c}\right), \ (x, t) \in \mathrm{VI}. \tag{49}$$

For the displacement in the other time-space region, it can be obtained by using the same procedure of time-space marching scheme. Since the boundary displacement at the end of right side is unknown, it is required to assume some unknown functions on the right-side boundary of full time-space region. In this way, $r_1(t)$ and $r_2(t)$ stand for the displacements of $u(L, t)$, $0 \le t \le L/c$ and $u(L, t)$,

$L/c \leq t \leq 2L/c$, respectively. After using the corresponding displacement representation to satisfy the boundary condition in Eq. (5), we have

$$EA \left. \frac{\partial u_{\mathrm{III}}(x,t)}{\partial x} \right|_{x=L} = -c_d \left. \frac{\partial u_{\mathrm{III}}(x,t)}{\partial t} \right|_{x=L}, \tag{50}$$

$$EA \left. \frac{\partial u_{\mathrm{VI}}(x,t)}{\partial x} \right|_{x=L} = -c_d \left. \frac{\partial u_{\mathrm{VI}}(x,t)}{\partial t} \right|_{x=L}. \tag{51}$$

Substituting Eq. (46) into Eq. (50) and using the displacement continuity for the displacement at $x = L$, $u_{\mathrm{III}}(L,0)$ and $u_{\mathrm{I}}(L,0)$, we have

$$r_1(t) = 0, \ 0 \leq t \leq L/c. \tag{52}$$

Similarly, substituting Eq. (49) into Eq. (51), the corresponding first-order ODE for $r_2(t)$ at the boundary of damper can be derived as

$$r_2'(t) = \frac{2EA}{EA + c_d c} a' \left(\frac{ct - L}{c} \right), \ L/c \leq t \leq 2L/c, \tag{53}$$

The general solution of Eq. (53) is

$$r_2(t) = \frac{2EA}{EA + c_d c} a \left(\frac{ct - L}{c} \right) + C_{r2}, \ L/c \leq t \leq 2L/c, \tag{54}$$

where the undetermined constant C_{r2} can be determined by satisfying the displacement continuity of solution in the intersection region IV and VI at $(x,t) = (L, L/c)$ as shown in Fig. 4.

3. AN ILLUSTRATIVE EXAMPLE

A finite bar with a boundary damper subjected to a support motion is considered as shown in Fig. 1. The model parameters are given: $c = 1m/s$, $EA = 1N$, $L = 7m$ and $c_d = 5N \cdot s/m$. By specifying the support motion,

$$a(t) = \sin(t), \tag{55}$$

the solutions of two approaches can be obtained as shown in the following subsection.

3.1 Mode superposition method

After substituting model parameters c, E, A, L, c_d and Eq. (55) into Eq. (40), the vibration response of displacement can be obtained by taking Eq. (40).

$$u(x,t) = \left(\frac{5 \left(e^{-\frac{1}{35}t} - \sin(t) - 35\cos(t) \right)}{1226} x + \sin(t) \right) + \sum_{n=-\infty}^{\infty} q_n(t) \left(e^{\lambda_n x} - e^{-\lambda_n x} \right), \tag{56}$$

where $q_n(t)$ is obtained by substituting model parameters c, E, A, L, c_d and Eq. (55) into Eq. (39).

According to the generalized Hooke's law, we can obtain the axial force as follows:

$$p(x,t) = AE \frac{\partial u(x,t)}{\partial x} = \left(\frac{5 \left(e^{-\frac{1}{35}t} - \sin(t) - 35\cos(t) \right)}{1226} \right) + \sum_{n=-\infty}^{\infty} q_n(t) \lambda_n \left(e^{\lambda_n x} + e^{-\lambda_n x} \right). \tag{57}$$

Since we assume $EA = 1\,N$ in the case, the space derivative of displacement is the axial force.

3.2 Method of characteristics in conjunction with the diamond rule

By substituting model parameters c, E, A, L, c_d and Eq. (55) into Eqs. (44)–(49), we have

$$u_{\mathrm{I}}(x,t) = 0, \ (x,t) \in \mathrm{I}, \tag{58}$$

$$u_{\mathrm{II}}(x,t) = \sin(t - x), \ (x,t) \in \mathrm{II}, \tag{59}$$

$$u_{\mathrm{III}}(x,t) = 0, \ (x,t) \in \mathrm{III}, \tag{60}$$

$$u_{\mathrm{IV}}(x,t) = \sin(t - x), \ (x,t) \in \mathrm{IV}, \tag{61}$$

$$u_{\mathrm{IV}}(x,t) = \sin(t - x), \ (x,t) \in \mathrm{V}, \tag{62}$$

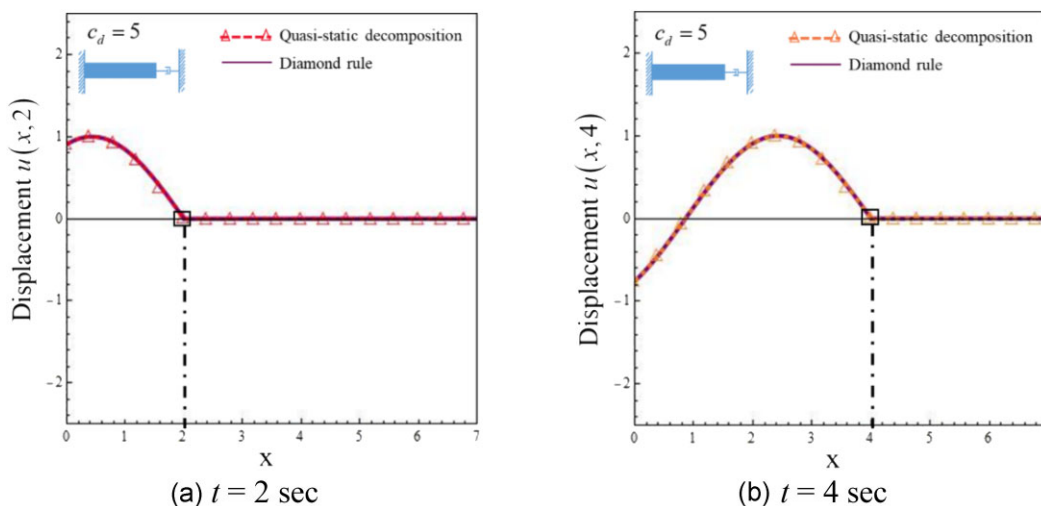(a) $t = 2$ sec   (b) $t = 4$ sec

Figure 5 Displacement profiles with the silent area by using the quasi-static decomposition (▲▬▬▲) and the diamond rule (——).

$$u_{VI}(x, t) = \sin(t - x) - \sin(x + t - 14) + r_2(x + t - 7), (x, t) \in VI. \tag{63}$$

where

$$r_2(t) = \frac{1}{3}\sin(t - 7), 7 \leq t \leq 14. \tag{64}$$

The space derivative of displacement of each region is

$$u'_I(x, t) = 0, (x, t) \in I, \tag{65}$$

$$u'_{II}(x, t) = -\cos(t - x), (x, t) \in II, \tag{66}$$

$$u'_{III}(x, t) = 0, (x, t) \in III, \tag{67}$$

$$u'_{IV}(x, t) = -\cos(t - x), (x, t) \in IV, \tag{68}$$

$$u'_V(x, t) = -\cos(t - x), (x, t) \in V, \tag{69}$$

$$u'_{VI}(x, t) = -\cos(t - x) - \cos(x + t - 14) + r'_2(x + t - 7), (x, t) \in VI. \tag{70}$$

The displacement profiles with the silent area for $t = 2$ and 4 s by using the mode superposition method and the diamond rule are shown in Fig. 5a and b, respectively. It is interesting to find that the mode superposition method of finite terms of series also yields the silent response. In Fig. 6, shadow regions, I and III, denote the dead zone. It matches the silent response begining at $x = 2$ and 4 m to the end of bar ($x = 7$ m), for the time when $t = 2$ and 4 s as shown in Fig. 5. It is found that the slope is discontinuous at $x = 2$ and 4 m for the time $t = 2$ and 4 s, respectively. These discontinuities occur at the locations of $(2,2)$ and $(4,4)$ in the x-t plane as shown in Fig. 6. In Fig. 6, the shadow region denotes the dead zone. As theoretically predicted, the discontinuity of the slope really occurs at the position of $(2,2)$ and $(4,4)$, on the characteristic line.

Regarding the non-silent area, the displacement profiles at $t = 8$ and 10 s are shown in Fig. 7a and b, respectively. It is also found that the slope is discontinuous at $x = 6$ and 4 m for the time $t = 8$ and 10 s, respectively. The axial force at $t = 8$ s is shown in Fig. 8. It is found that the axial force is discontinuous at $x = 6$ m, and it is corresponding to the slope of displacement at $x = 6$ m for the time $t = 8$ s in Fig. 7a. The zoom view of the local profile of axial force with a jump by using the quasi-static decomposition approach and the method of the diamond rule are shown in Fig. 9. It is found that the mode superposition approach presents the Gibbs phenomenon. These slope discontinuities occur at the locations of $(6,8)$ and $(4,10)$ in the x-t plane as shown in Fig. 10. This finding matches well from the mathematical requirement that the discontinuity can only occur at the position on the characteristic line [21].

The displacement response at $x = 5$ m by using the mode superposition method and the diamond rule are shown in Fig. 11. To test the convergence of the mode superposition method, the plots of displacement profile and the time history with different numbers of
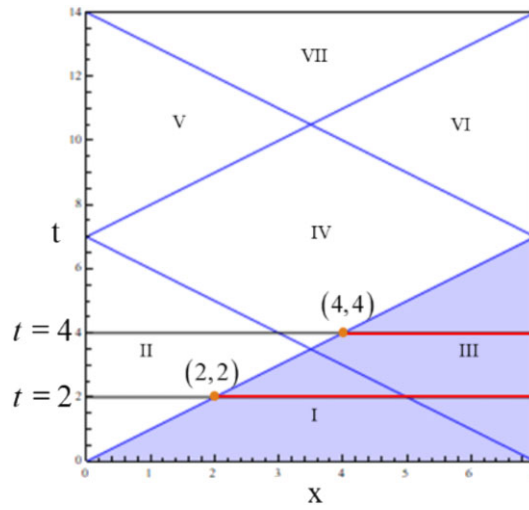
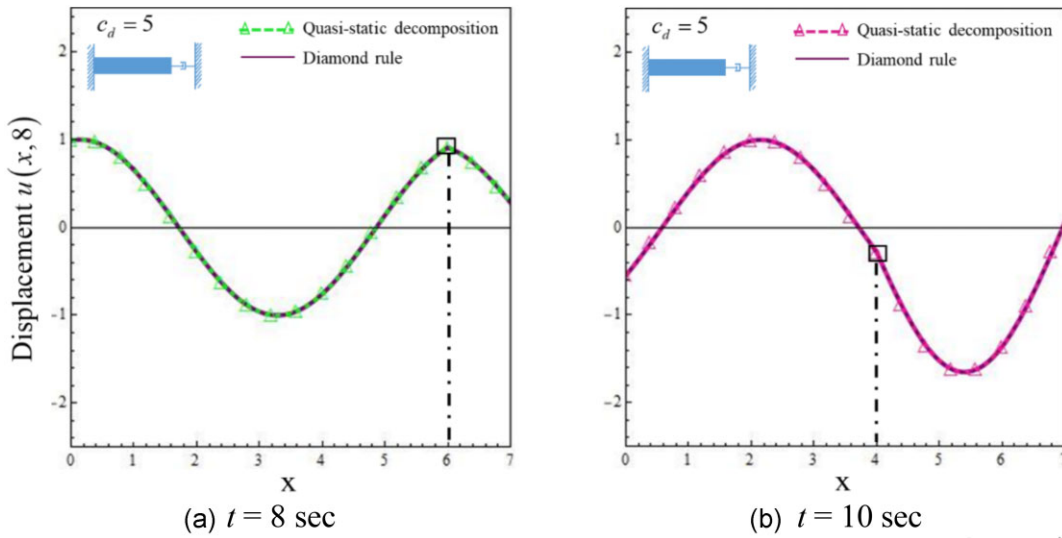**Figure 6** The locations of slope discontinuities at $(2,2)$ and $(4,4)$.

(a) $t = 8$ sec   (b) $t = 10$ sec

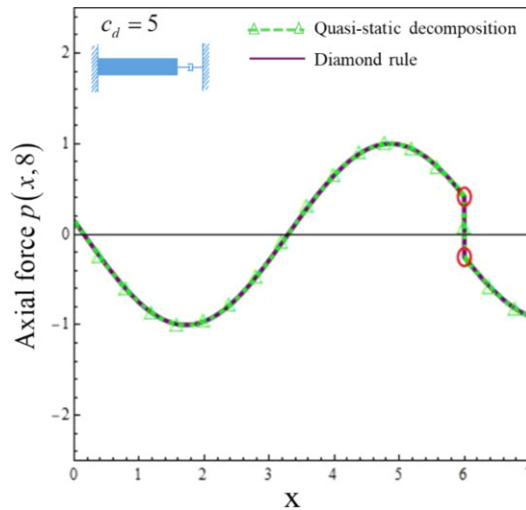**Figure 7** Displacement profiles by using the quasi-static decomposition (△──△) and the diamond rule (──).

Figure 8 Profile of the axial force at $t = 8$ by using the quasi-static decomposition (△──△) and the diamond rule (──).

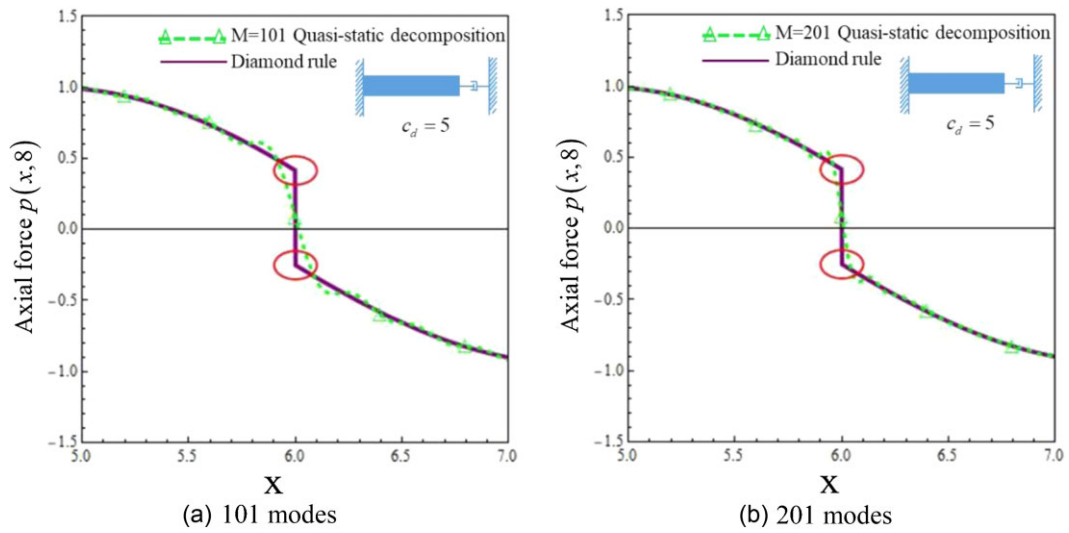**Figure 9** Local profile of the axial force at t = 8 by using the quasi-static decomposition (△– –△) and the diamond rule (———).
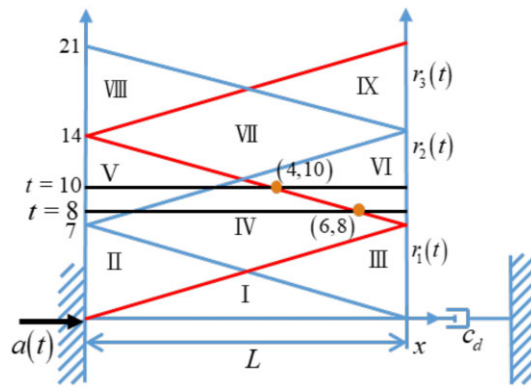
Figure 10 The locations of slope discontinuities at $(6,8)$ and $(4,10)$.

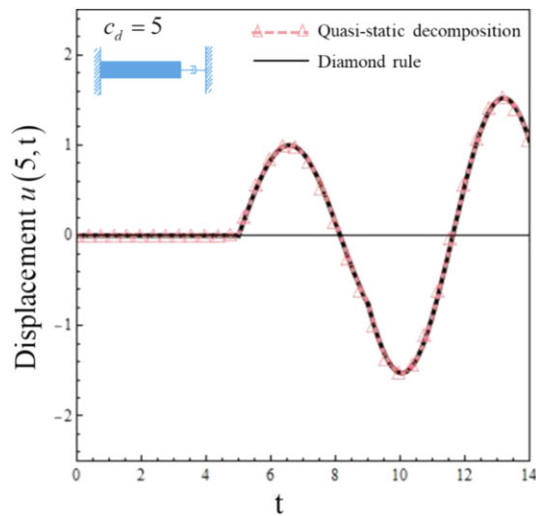**Figure 11** Displacement history at $x = 5$ m by using the quasi-static decomposition (△– –△) and the diamond rule (———).

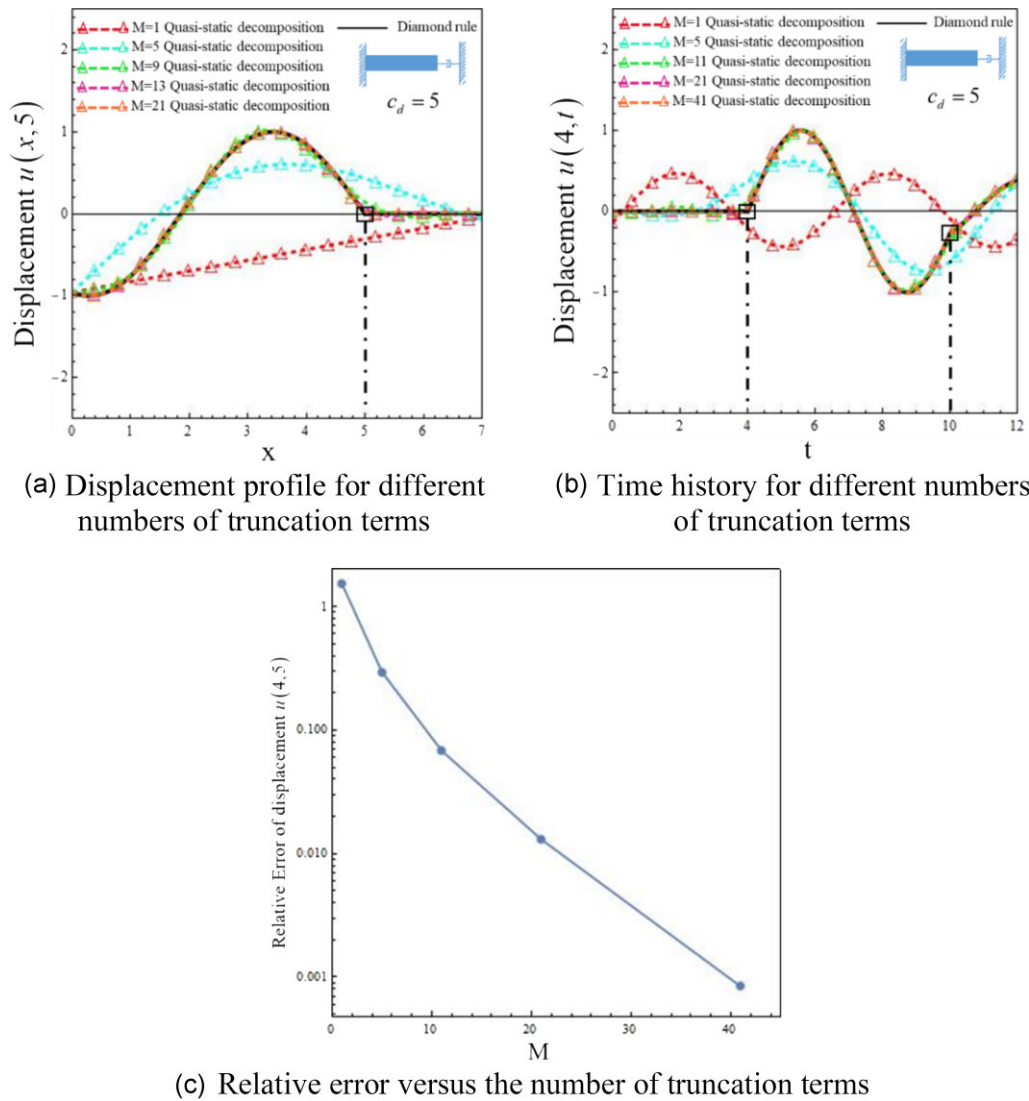(a) Displacement profile for different
numbers of truncation terms

(b) Time history for different numbers
of truncation terms

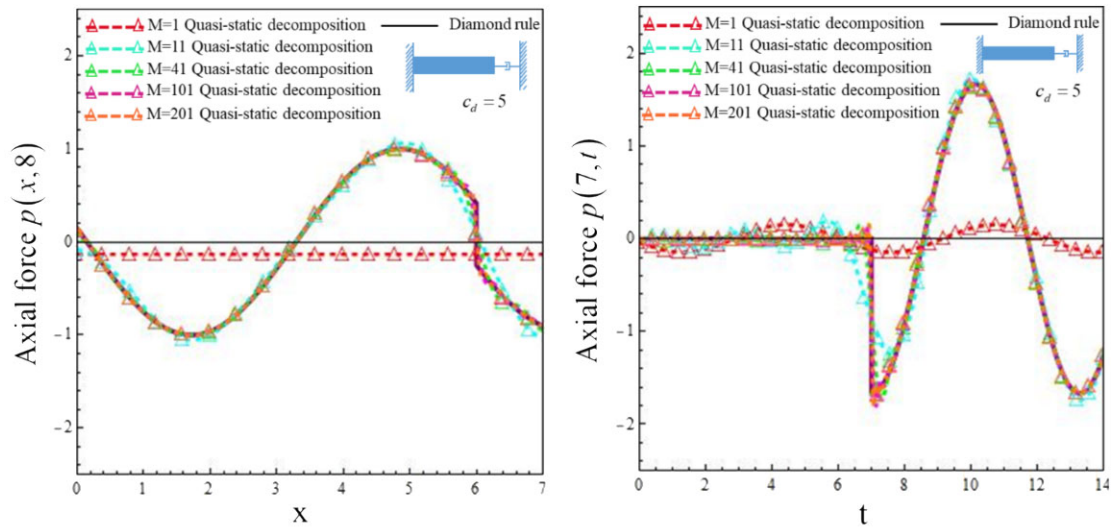(c) Relative error versus the number of truncation terms

Figure 12 Convergence tests: (a) displacement profile, (b) time history, (c) relative error.

truncation terms are shown in Fig. 12a and b. The relative error obtained by using the mode superposition method versus the number of truncation terms is also shown in Fig. 12c. The exact solution is calculated as a reference by using the diamond rule. It found that adopting $M = 41$ modes can reach the maximum relative error of 0.1%.

Additionally, to test the convergence of the axial force by the termwise spatial differentiation with respect to the displacement in the mode superposition method, the plots of profile of axial force and the history of axial force with different numbers of truncation terms are shown in Fig. 13a and b. The relative error of axial force obtained by using the mode superposition method versus the number of truncation terms is also shown in Fig. 13c. The definition of relative error is defined by $\left| \frac{p^{\text{Mode}}(7,8) - p^{\text{Diamond}}(7,8)}{p^{\text{Diamond}}(7,8)} \right|$, where the superscript of $p(7, 8)$ is denoted by the corresponding approach.

From Table 1, it is found that the numerical results satisfy the boundary condition when the number of the truncation terms is over 51. In order to check the boundary condition of the damper, numerical results of the axial force and damping force in equilibrium are given in Table 1.

The convergence test of S_M (only the series summation without the quasi-static part) and its derivative with respect to x at the position $x = 0.6L$, $0.97L$ and L for $t = 8$ and 10 are shown in Tables 2 and 3, respectively. Additionally, the convergence tests of series summation (S_M and S'_M) at $(x, t) = (6, 8)$ and $(4, 10)$ are also done and are discussed in Table 4. For the above cases of no jump, uniform convergence is confirmed. There is a jump for the axial force when (x, t) is on the characteristic line. We check $(x, t) = (6, 8)$ and $(4, 10)$ as shown in Fig. 10. For the axial force in Table 4, the jump of axial force can be exactly captured in different regions using the method of diamond rule, while the mode superposition method yields only one value in the mean. In this case, the mode superposition method converges to the solution piecewisely.

(a) Profile of the axial force for different numbers of truncation terms

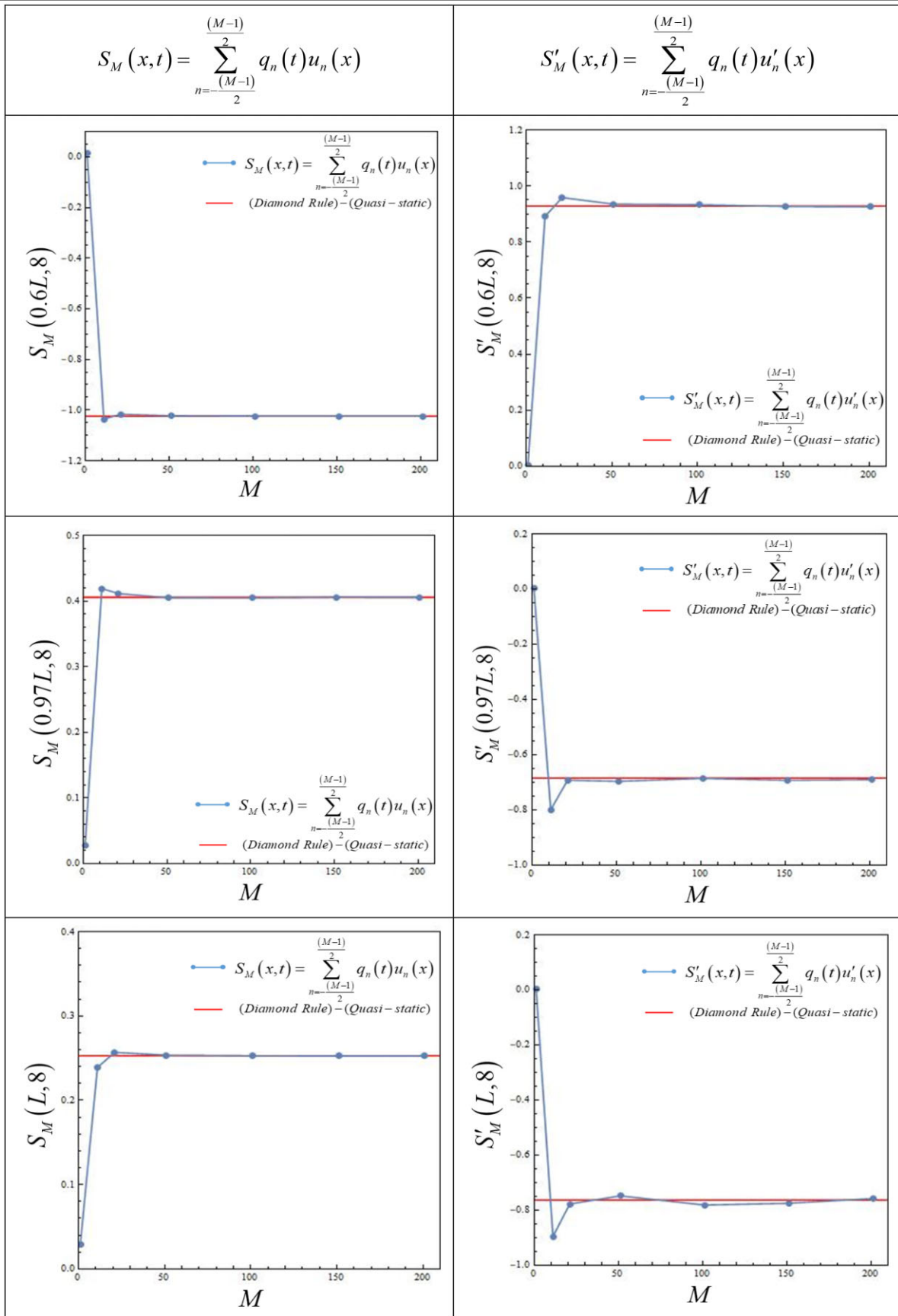(b) History of the axial force for different numbers of truncation terms
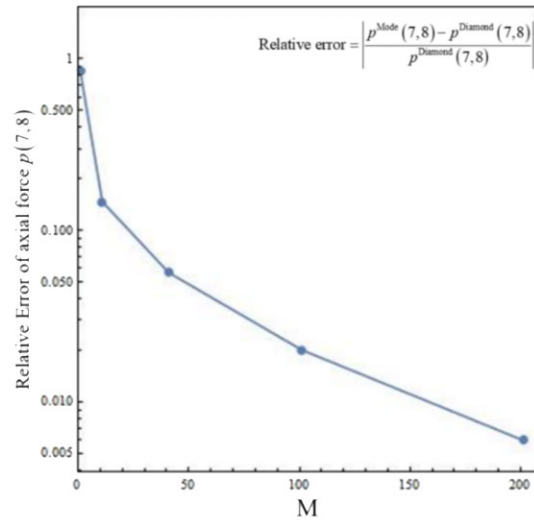
(c) Relative error versus the number of truncation terms

Figure 13 Convergence tests: (a) profile of the axial force, (b) history of the axial force, (c) relative error.

Table 1 Numerical results to check the viscously boundary condition.

	$c = 1m/s, EA = 1N, L = 7m, c_d = 5N \cdot s/m, x = L$ and $t = 10$	
Number of truncation terms (M)	**Axial force of Eq. (5)** $EA\frac{\partial u(x,t)}{\partial x}\big|_{x=L}$	**Damping force of Eq. (5)** $-c_d\frac{\partial u(x,t)}{\partial t}\big|_{x=L}$
1	0.113788	0.706723
11	1.716176	1.69778
51	1.63705	1.63506
101	1.65378	1.65325
201	1.6465	1.6462
501	1.64944	1.64931
1001	1.65006	1.64999

Table 2 Convergence test of S_M and S'_M $(t = 8)$

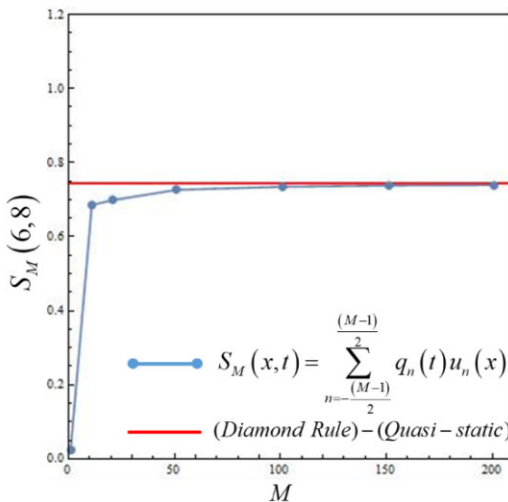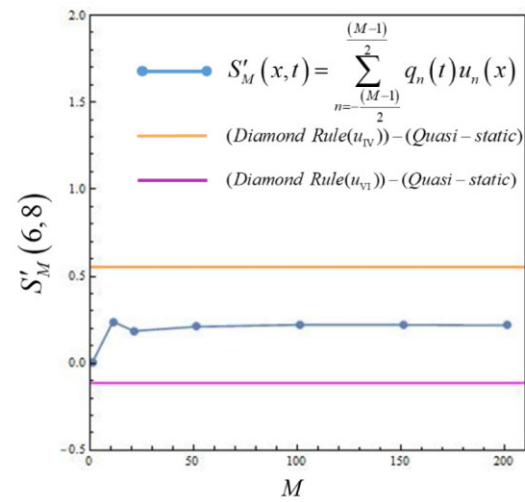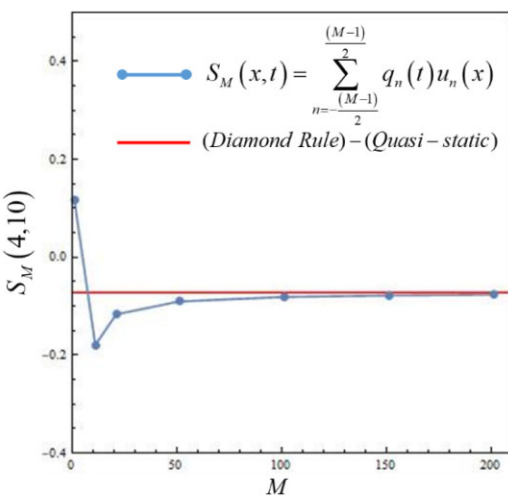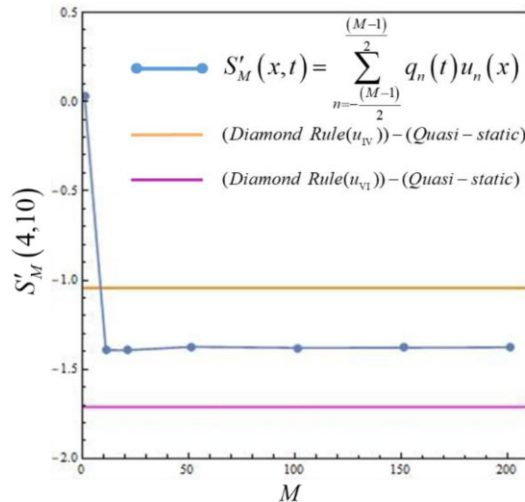| $S_M(x,t) = \sum\limits_{n=-\frac{(M-1)}{2}}^{\frac{(M-1)}{2}} q_n(t)u_n(x)$	$S'_M(x,t) = \sum\limits_{n=-\frac{(M-1)}{2}}^{\frac{(M-1)}{2}} q_n(t)u'_n(x)$

Table 3 Convergence test of S_M and S'_M ($t = 10$)

Table 4 Convergence test of S_M and S'_M at $(x, t) = (6, 8)$ and $(4, 10)$

$$S_M(x,t) = \sum_{n=-\frac{(M-1)}{2}}^{\frac{(M-1)}{2}} q_n(t)u_n(x)$$	$$S'_M(x,t) = \sum_{n=-\frac{(M-1)}{2}}^{\frac{(M-1)}{2}} q_n(t)u'_n(x)$$

4. CONCLUSIONS

Regarding the longitudinal vibration, a finite bar with a viscously damped boundary is a non-conservative system. Since the two initial conditions are homogeneous and the external force is zero, this finite bar is excited by a support motion at the clamped end. In addition, this problem is also a direct problem. Not only the mode superposition approach but also the method of characteristics was employed to solve the problem. From the viewpoint of computation, the complex-mode approach may not be simpler and easier than employing the FEM. However, it provides a benchmark to interpret FEM results. Our second approach as known as the diamond rule is both easy and simple and is highly recommended to scientists and engineers. For the mode superstition method, the orthogonality of complex modes was achieved after special treatment. The diamond rule and the mode superposition method were both independently employed to derive an exact solution and a series solution, respectively. The positions of the slope discontinuity on the specified characteristic line can be mathematically predicted and numerically verified by using the diamond rule and mode superposition method, respectively. After comparing the results calculating by using two methods, good agreements are made. In addition, the displacement response can be straightforwardly calculated in the space-time domain by using the diamond rule without considering the separation variables of space and time. In this way, using the diamond rule to solve the problem of non-conservative system with a damper is easier than using the mode superposition method, since it is free to consider the complex-valued eigen system. For clarity, comparisons between two methods, for advantages and disadvantages, are summarized in Table 5.

Table 5 Comparison of the two approaches for the vibration problem of a finite bar

Item analysis Solution form	Method	
	Mode superposition method in conjunction with the quasi-static decomposition Series solution	**Method of characteristics in conjunction with the diamond rule** Exact solution
Advantage	1. Free of dividing the space-time region to represent the corresponding displacement response 2. The vibration response can be directly obtained without any difficulty for any time and position	1. Free of the truncation error of finite term of series sum 2. It can easily capture the dead zone 3. General approach for either conservative or non-conservative system 4. Suitable for support excitation of short duration, e.g. earthquake input
Disadvantage	1. Error due to a finite truncation series in the real computation 2. Convergence test is required 3. Complex-valued eigenvalues and eigenequation are required for a damped system 4. Orthogonality condition needs special care	Previous stage error propagates to the later response

Chen JT:

Since 1980, I was an undergraduate student of Dept. of Civil Engineering, NTU, Prof. Yeh was the Head of the Department. During the summer vacation of that time, he always asked me to read some books, e.g. the book of Greenberg on Green's Function and the book of Y. C. Fung on continuum mechanics. In 1984, he encouraged me to study at the Institute of Applied Mechanics, NTU founded at the same time by Prof. Y. H. Pao and Prof. C. S. Yeh. After working at the CSIST for 4 years, I returned NTUCE to fulfill my PhD. degree. At that time, I attended his courses on elasticity and was his teaching assistant. I co-authored with him two SCI papers, Communications in Numerical Methods in Engineering and Earthquake Engineering & Structural Dynamics in 1995 and 1996, respectively. He showed me his interest on the vibration problem of this paper and asked me to do this homework. I am very sorry to have some results after near 30 years until now. However, it is too late to show him the analytical solution. Now the only thing that I can do is to contribute this paper in the memorial issue of JOM for him. I am proud of being his student, teaching assistant and co-author for some journal and conference papers.

Kao HC:

It's my honor that I can solve the problem that Prof. Yeh was interested. However, it's sad that I have no chance to show this article to him because he passed away on May, in 2022. I appreciate his contribution on structural engineering and earthquake engineering. Although I haven't met him before, he has a great influence on young generation in structural and earthquake engineering. As a master student, I will follow his step and continue to pay effort on earthquake engineering.

Lee JW:

In 2009, I was a master student and attended the student paper competition of the 33rd National Conference on Theoretical and Applied Mechanics. Due to the help by NTOU/MSV group and the guidance from my advisor Prof. J.T. Chen, I finally won the first place. This result encouraged me, and stimulated my academic career. Especially, Prof. Yeh was the award presenter at that time. It is honor to me. It always reminded me to do my best on my research.

Lee YT:

In my memory, I attended the student paper competition of the 32nd National Conference on Theoretical and Applied Mechanics and won the first place. Prof. Yeh was the award presenter. When he awarded the certificate of merit to me, he was also glad to tell me that my advisor (Prof. J. T. Chen) was his former student. At that time, I thought that Prof. Yeh may feel honor because the student of his student can win this award. This also encouraged me to do better research in the future.

APPENDIX

The nth complex-valued eigenfunction and complex-valued eigenvalue can be deduced from the free vibration in conjunction with the boundary conditions.

The governing equation for the free vibration problem of a finite bar is as follows:

$$c^2 \frac{\partial^2 u(x,t)}{\partial x^2} = \frac{\partial^2 u(x,t)}{\partial t^2}, \quad 0 < x < L, t > 0. \tag{A1}$$

The boundary condition at the left-hand side $(x = 0)$ can be expressed by the fixed end as follows:

$$u(0, t) = 0. \tag{A2}$$

The boundary condition containing a damper at the right hand side is given as follows:

$$EA \frac{\partial u(x,t)}{\partial x}\bigg|_{x=L} = -c_d \frac{\partial u(x,t)}{\partial t}\bigg|_{x=L}. \tag{A3}$$

The solution can be separated in terms of a product of space and time functions or called the method of separation variables as follows:

$$u(x, t) = X(x) T(t), \tag{A4}$$

where $X(x)$ is the space function and $T(t)$ is the generalized coordinates. By substituting Eq. (A4) into Eq. (A1), we have two ordinary differential equations,

$$\frac{d^2 X(x)}{dx^2} - \lambda^2 X(x) = 0, \tag{A5}$$

and

$$\frac{d^2 T(t)}{dt^2} - \lambda^2 c^2 T(t) = 0, \tag{A6}$$

where λ is the complex-valued eigenvalue.

From Eq. (A2) and Eq. (A5), we have

$$X(x) = \left(e^{\lambda x} - e^{-\lambda x}\right). \tag{A7}$$

The general solution to Eq. (A6) is

$$T(t) = Ge^{\lambda ct} + He^{-\lambda ct}. \tag{A8}$$

Applying the viscous boundary condition of Eq. (A3) to Eqs. (A7) and (A8), we have

$$EA\left[\lambda\left(e^{\lambda L} + e^{-\lambda L}\right)e^{\lambda ct}\right] = -c_d\left[\lambda c\left(e^{\lambda L} - e^{-\lambda L}\right)e^{\lambda ct}\right]. \tag{A9}$$

Rearranging Eq. (A9), we have

$$-\frac{EA}{c_d c} = \frac{e^{\lambda L} - e^{-\lambda L}}{e^{\lambda L} + e^{-\lambda L}}, \tag{A10}$$

and $H = 0$.

We can rewrite the right-hand side of Eq. (A10),

$$-\frac{EA}{c_d c} = \tanh(\lambda L). \tag{A11}$$

By using the complex trigonometric function to rewrite the hyperbolic function of Eq. (A11), we obtain

$$-\frac{EA}{c_d c} = -i\tan(i\lambda L). \tag{A12}$$

Rearranging Eq. (A12), we have

$$\tan(i\lambda L) = \frac{EA}{ic_d c}. \tag{A13}$$

By taking the arctangent operator to Eq. (A13), we have

$$i\lambda_n L = \arctan\left(\frac{EA}{ic_d c}\right) + n\pi, \quad n = 0, \pm 1, \pm 2, \cdots. \tag{A14}$$

Rearranging Eq. (A14), we obtain

$$\lambda_n = \frac{-i}{L}\arctan\left(\frac{EA}{ic_d c}\right) - \frac{n\pi}{L}i, \quad n = 0, \pm 1, \pm 2, \cdots. \tag{A15}$$

By using the function of $\arctan(x) = \frac{1}{2i}\ln\left(\frac{1+ix}{1-ix}\right)$ to rewrite the inverse trigonometric function of Eq. (A15), we obtain

$$\lambda_n = -\frac{1}{2L}\ln\left(\frac{c_d c + EA}{c_d c - EA}\right) - \frac{n\pi}{L}\mathrm{i}, \, n = 0, \, \pm 1, \, \pm 2, \cdots. \tag{A16}$$

REFERENCES

1. Oliveto G, Santini A, Tripodi E. Complex modal analysis of a flexural vibrating beam with viscous end conditions. *Journal of Sound and Vibration* 1997; **200**: 327–345.
2. Hull AJ. A closed form solution of a longitudinal bar with a viscous boundary condition. *Journal of Sound and Vibration* 1994; **169**: 19–28.
3. Singh R, Lyons WM, Prater G. Complex eigenvalue for longitudinal vibration bars with a viscously damped boundary. *Journal of Sound and Vibration* 1989; **133**(2): 364–367.
4. Chen JT, Jeng YS. Dual series representation and its applications a string subjected to support motions. *Advances in Engineering Software* 1996; **27**: 227–238.
5. Chen JT, Kao HC, Lee YT, Lee JW. Support motion of a finite bar with an external spring. *Journal Low Frequency Noise Vibration Active Control*, 2022; **41**(3): 1014–1029.
6. Chen JT, Hong HK, Yeh CS, Chyuan SW. Integral representations and regularization for a divergent series solution of a beam subjected to support motion. *Earthquake Engineering & Structural Dynamics* 1996; **25**: 909–925.
7. Chen JT, Chou KS, Kao SK. One-dimensional wave animation using Mathematica. *Computer Applications in Engineering Education* 2009; **17**: 323–339.
8. Zhao L, Chen Q. Neumann dynamic stochastic finite element method of vibration for structures with stochastic parameters to random excitation. *Computers & Structures* 2000; **77**: 651–657.
9. Albuquerquea EL, Sollero P, Fedelinski P. Free vibration analysis of anisotropic material structures using the boundary element method. *Engineering Analysis with Boundary Elements* 2003; **27**: 977–985.
10. Li H, Wang QX, Lam KY. Development of a novel meshless Local Kriging (LoKriging) method for structural dynamic analysis. *Computer Methods in Applied Mechanics and Engineering* 2004; **193**: 2599–2619.
11. Su YC, Cho TY. Free vibration of a single-walled carbon nanotube based on the nonlocal Timoshenko beam model. *Journal of Mechanics* 2021; **37**: 616–635.
12. Lin F, Peng JS, Xue SF, Yang L, Yang J. Nonlinear free vibration of size-dependent microbeams with nonlinear elasticity under various boundary conditions. *Journal of Mechanics* 2021; **37**: 380–403.
13. Jovanovic V. A Fourier series solution for the transverse vibration response of a beam with a viscous boundary. *Journal of Sound and Vibration* 2011; **330**: 1504–1515.
14. Jovanovic V. A Fourier series solution for the transverse vibration of a clamped beam with a torsional damper at the boundary. *Journal of Vibration and Control* 2011; **18**(3): 344–356.
15. Udawadia FE. On the longitudinal vibrations of a bar with viscous boundaries Super-stability super-instability and loss of damping. *International Journal of Engineering Science* 2012; **50**: 79–100.
16. Jovanovic V. A Fourier series solution for the longitudinal vibrations of a bar with viscous boundary conditions at each end. *Journal of Engineering Mathematics* 2013; **79**: 125–142.
17. Gurgoze M, Erol H. Dynamic response of a viscously damped cantilever with a viscous end condition. *Journal of Sound and Vibration* 2006; **298**: 132–153.
18. Farlow SJ. *Partial Differential Equations for Scientists and Engineers.* Canada: John Wiley and Sons, 1937.
19. Wilkinson DH, Curtis EM. *Water Hammer in a Thin Walled Pipe,* Proceedings of the 3rd International Conference on Pressure Surges, BHRA, Canterbury, UK. 221–240, 1980.
20. John F. *Partial Differential Equation,* 2th edn. New York: Springer-Verlag, 1975.
21. Carrier GF, Pearson CE. *Partial Differential Equations: Theory and Technique,* 1st edn. New York: Academic Press, 1976.